Biochimica et Biophysica Acta 1850 (2015) 1120–1130

Contents lists available at ScienceDirect

Biochimica et Biophysica Acta

journal homepage: www.elsevier.com/locate/bbagen

Glucose 6-phosphate and alcohol dehydrogenase activities are components of dynamic macromolecular depots structures

Angela Tramonti [a], Michele Saliola [b,*]

[a] Istituto di Biologia e Patologia Molecolari, CNR-Dipartimento di Scienze Biochimiche "Rossi Fanelli", Sapienza Università di Roma, Piazzale Aldo Moro 5, 00185 Rome, Italy
[b] Dipartimento di Biologia e Biotecnologia "C. Darwin", Sapienza Università di Roma, Piazzale Aldo Moro 5, 00185 Rome, Italy

ARTICLE INFO

Article history:
Received 21 October 2014
Received in revised form 23 January 2015
Accepted 30 January 2015
Available online 7 February 2015

Keywords:
In gel-native assay
Mass spectrometry
Depots
NAD(P)$^+$/NAD(P)H redox balance

ABSTRACT

Background: Membrane-associated respiratory complexes, purinosome and many intracellular soluble activities have reported to be organized in dynamic multi-component macromolecular complexes using native PAGE, 2D SDS-PAGE, electron and systematic microscopy and genome-wide GFP fusion library.
Methods: In-gel staining assays, SDS-PAGE and LC–MSMS techniques were performed on cellular extracts to analyze, isolate and identify the proteins associated with glucose 6-phosphate dehydrogenase (G6PDH) and fermentative alcohol dehydrogenase (ADH) I isoform in both *Kluyveromyces lactis* and *Saccharomyces cerevisiae* yeasts.
Results: Analysis of LC–MSMS data showed that a large number of components, belonging to glycolysis, pentose phosphate, folding and stress response pathways, were associated with G6PDH and Adh1 putative complexes and that a number of these proteins were identical in either network in both yeasts. However, comparison of in-gel staining assays for hexokinase, phosphoglucoisomerase, acetaldehyde dehydrogenase, ADH and G6PDH showed that, despite their identification in these structures, functional localization of these activities varied according to growth conditions and to NAD(P)$^+$/NAD(P)H redox ratio.
Conclusions: Reported data show that intracellular proteins are organized in large dynamic 'depots' and the NAD(P)$^+$/NAD(P)H redox balance is one of the major factors regulating the assembly and the re-assortment of components inside the different metabolic structures.
General significance: The aim of this work is directed towards the comprehension of the mechanisms involved in the assembly, organization, functioning and dynamic re-assortment of cellular components according to physiological and/or pathological conditions.

1. Introduction

Most cellular processes are carried out by protein complexes [1], which provide increased reaction efficiency, metabolite channeling and coordinated control of reaction rates. Many complexes have been characterized and the 3D structure determined for a few of them: the fatty acid synthase complex is just an example [2]. Many, if not all, complexes in turn can assemble in dynamic multi-component macromolecular networks, called "depots" [3,4]. In these networks, individual components can be transiently held and released, migrate away from a complex or participate to multiple spatial and functional distinct depots according to cellular needs. Moreover, each component may be inactive in a complex and become functional upon release, or may have the same or different function in and out of the complex [3]. Many reports have provided evidence for the existence of these supra-molecular structures, among them tRNA multisynthetase complex, the purinosome and the ribosome [5–7]. Experimental studies using affinity purification and mass spectrometry aiming at to define the interactome in *Saccharomyces cerevisiae* have shown that in this organism more than 500 protein complexes exist and most of these complexes have a component in common with at least one other multi-protein assembly [8,9]. The organization of macromolecules in dynamic depots may play important roles during the cell cycle [10] and also during stationary phase, when a large number of metabolic proteins form reversible macroscopic foci inside quiescent cells [11]. Re-entry into proliferating conditions when nutrients are made available requires a large-scale reprogramming of the metabolic and replicatory machinery held in poised state during quiescence. Systematic microscopy tracking of proteins and genome-wide GFP fusion library has shown that in this condition a large-scale reorganization of components in the complexes occurs. Several tagging methods have been used to detect and analyze single multi-protein complex speculating that the large-scale reorganization of components may

Abbreviations: ADH, alcohol dehydrogenase; Eno, enolase; G6PDH, glucose 6-phosphate dehydrogenase; PPP, pentose phosphate pathway; LC–ESI-MSMS, liquid chromatography–electrospray ionization-tandem mass spectrometry

* Corresponding author. Tel.: +39 06 49912544; fax +39 06 49912351.
E-mail addresses: angela.tramonti@uniroma1.it (A. Tramonti), michele.saliola@uniroma1.it (M. Saliola).

http://dx.doi.org/10.1016/j.bbagen.2015.01.021
0304-4165/

function a) to improve catalytic efficiency, b) as storage depots and c) to aggregate dysfunctional/unfolded proteins [11,12].

In the present work we used native polyacrylamide gels electrophoresis (PAGE), staining assays, SDS-PAGE, analysis of mutants and LC–MSMS techniques to separate, isolate and identify the proteins associated with glucose 6-phosphate dehydrogenase (G6PDH) and the fermentative alcohol dehydrogenase (ADH) I isoform. These two key enzymes, located at crucial glycolysis/PPP and glycolysis/fermentation routes, provide NADPH for biomass synthesis/response to stress and to reoxidize the NADH necessary to feed glycolytic flux, respectively, in both *Kluyveromyces lactis* and *S. cerevisiae* yeasts.

G6PDH, an evolutionary conserved protein [13,14], catalyzes the rate-limiting NADPH producing step of the pentose phosphate pathway (PPP) [15]. In the yeast *K. lactis* this enzyme has been detected, on native PAGE, as two differently migrating forms [16] representing different oligomeric states of the enzyme determined by cytosolic accumulation of NAD(P)H [17].

G6PDH oligomers, as well as Adh1, were singularly cut, eluted and purified from native gels and then analyzed on SDS-PAGE. Surprisingly, a large number of almost identical proteins in different growth conditions were found to be associated with G6PDH and Adh1 in both *K. lactis* and *S. cerevisiae* yeasts. These proteins were identified by mass spectrometry as glycolytic, PPP, folding, stress response related proteins and other components of the cellular/cytoskeleton structures. The presence of different intracellular complexes containing a relevant number of common components suggested the participation of these proteins in multiple functional distinct networks. Specific staining assays for components of these macromolecular structures led us to the conclusion that they are organized into dynamic "depots", whose components can be active or inactive depending on the growth under physiological/pathological conditions.

2. Materials and methods

2.1. Strains, media and culture conditions

The *K. lactis* strains used in this work are reported in Table 1. Media preparations and cultures conditions were performed as previously described [18].

2.2. ADH, ALD, G6PDH, HXK and PGI in-gel staining assays

K. lactis cell extract preparation, clear native PAGE, electrophoresis conditions and ADH and G6PDH staining assays were carried out as previously described [16,18]. G6PDH in vitro assay has been previously described [16].

In-gel staining assay for aldehyde dehydrogenase (ALD) was performed as described for ADH but with longer incubation times, with the following staining mixtures ($NADP^+$-dependent): 20 μl $NADP^+$, 30 μl NTB, 15 μl PMS, 5 μl 3 M CH_3COOK, 50 μl acetaldehyde 10% (v/v), and H_2Odd to 5 ml; (NAD^+-dependent): 30 μl NAD^+, 30 μl NTB (Nitrotetrazolium Blue), 15 μl PMS (Phenazine Methosulfate), 5 μl $MgCl_2$ 1 M, 50 μl acetaldehyde 10% (v/v), and H_2Odd to 5 ml. Stock solutions for NAD^+, $NADP^+$, NTB and PMS were as previously described [16,18].

In-gel phosphoglucose isomerase (Pgi) and hexokinase (Hxk) staining assays were performed placing, after the removal of one of the glasses, the native run gel on a polymerized polyacrylamide gel containing the staining mixture. Staining gel for PGI: 0.8 ml acrylamide/bis 40% (w/v) solution, 2.0 ml TE buffer (10 mM Tris–HCl, pH 8.0, 1 mM EDTA), 2.4 ml H_2Odd, 40 μl $NADP^+$, 40 μl NTB, 25 μl PMS, 5 μl 1 M $MgCl_2$, 40 μl fructose 6-P (100 mg/ml), 600U G6PDH (yeast), 50 μl 10% (w/v) ammonium persulfate and 6 μl TEMED. Staining gel for HXK: 0.8 ml acrylamide/bis 40% (w/v) solution, 2.0 ml TE, 2.4 ml H_2Odd, 40 μl $NADP^+$, 40 μl NTB, 25 μl PMS, 50 μl glucose (100 mg/ml); 500 μl ($NADP^+$, ATP and magnesium sulfate in triethanolamine buffer solution pH 7.6) (from r-biopharm D-glucose kit cat. 10716251035), 50 μl 10% ammonium persulfate and 6 μl TEMED.

Table 1
Yeast strains used in this study.

K. lactis	Genotype	Reference
CBS2359	*MAT**a***	CBS collection
GG1996	*MAT**a** rag2Δ*	[17]
MW179-1D	*MATα metA1 ade-T600 leu2 trpA1 ura3 lac4*	[17]
MS7-62	*MATα lysA1 argA1 adh1Δ adh2Δ adh3Δ adh4Δ*	[17]
MS7-62/ADH1	*MATα lysA1 argA1 adh2Δ adh3Δ adh4Δ*	[17]
MW270-7B	*MAT**a** metA1 leu2 ura3*	[19]
MW270-7B/eno1Δ	*MAT**a** metA1 leu2 ura3 eno1Δ*	[19]
JA6/dgr151	*MATα ade1ade2 trp1-11 adh3 rag5*	[20]
PM6-7A	*MAT**a** ade-T600 uraA1-1 adh3*	[21]
PM6-7A/rag6	*MAT**a** ade-T600 uraA1-1 adh3 rag6Δ*	[21]
PM6-7A/tpi1Δ	*MAT**a** ade-T600 uraA1-1 adh3 tpi1Δ*	[22]
MW98-8C	*Matα lysA1 argA1 ura3 rag1 rag2*	[23]
MW98-8C/pgk1Δ	*Matα lysA1 argA1 ura3 rag1 rag2 pgk1Δ*	[23]
S. cerevisiae		
BY4741	*MAT**a** hys3Δ0 leu2Δ0 met15Δ0 ura3Δ0*	Euroscarf

2.3. Determination of ADH and G6PDH enzymatic activities

ADH activity was assayed by measuring the rate of NAD^+ reduction/NADH reoxidation at 340 nm in 50 mM Tris–HCl, pH 8.0 buffer containing either ethanol (200 mM) or acetaldehyde (20 mM) as a substrate. G6PDH activity was assayed by measuring the rate of $NADP^+$ reduction at 340 nm in 0.1 M Tris–HCl buffer, pH 8.8, containing 10 mM $MgCl_2$, 0.1 mM glucose-6-phosphate and 0.1 mM $NADP^+$.

2.4. Elution and analysis of stained G6PDH and Adh1 bands from native PAGE

The stained bands on native PAGE were cut and the proteins extracted from the bands with extraction devices (Millipore), concentrated and washed with TE buffer using 10 kDa MWCO ultrafiltration tools (Vivaspin, Sartorius). About 2 μg of proteins were finally yielded from 2 to 2.5 mg of total soluble proteins fractionated on native PAGE.

The G6PDH-specific band eluted from native PAGE was analyzed on size exclusion column (Superdex 200; GE Healthcare) for FPLC experiments equilibrated with Tris–glycine buffer and calibrated with ferritin (440 kDa), conalbumin (75 kDa), bovine serum albumin (67 kDa) and RNase A (13.7 kDa).

The identification of proteins within G6PDH and Adh1 native PAGE extracted bands was performed by nanoLC–ESI-MSMS by a custom service (Proteome Factory). The mass spectral data were interpreted with Mascot software. In the supplementary tables (S1–S7) we reported the results of all protein identifications, with the score (combination of scores of all observed mass spectra that can be matched to amino acid sequences within that protein), the number of identified peptides per protein, and emPAI (Exponentially Modified Protein Abundance Index), an index that indicates the protein content on the basis on the ratio of the number of observed peptides to the number of observable peptides [24]. From these data we have pulled out the proteins with high score and high emPAI presented in summary in Tables 2, 3 and 4.

2.5. SDS-PAGE analysis and western blot

Protein samples were run on a 12% SDS-PAGE and transferred onto PVDF membranes (Immobilon; Millipore) using the mini Trans-Blot Electrophoretic Transfer Cell (Bio-Rad). Membranes were probed with anti-G6PDH (LifeSpan Biosciences), anti-enolase (anti-Eno; Santa cruz Biotechnology), anti-triosephosphate isomerase (anti-Tpi; Nordic Immunology Laboratories) and anti-3-phosphoglycerate kinase (Molecular Probes) polyclonal antibodies.

Table 2
Proteins identified in the G6PDH and G6PDH/GFP bands (S and I) by nanoLC–ESI-MSMS digested with trypsin or chymotrypsin (CHT) from *K. lactis* glucose- (D) and glycerol- (G) extracts.

Uniprot	Protein name	S_D	S_D CHT	I_D	S_G	S_{GGFP} CHT
PPP/related activities						
P48828	Zwf1-Glucose-6-P dehydrogenase	+	+	+	+	+
Q6CMI0	Met6-Cobalamin-indep methionine synthase	+	+	+	+	+
Q92441	Met17-O-acetylserine /O-acetylhomoserine sulf.	+	+	+		
P34214	Tal1-Transaldolase	+	+	+	+	+
O13474	Ura5-Orotate phosphoribosyltransferase		+	+	+	
Q6CYD7	Sah1-Adenosylhomocysteinase	+	+	+	+	+
Q6CKK3	Aro8-Aromatic aminotransferase	+	+	+	+	
Q6CTY8	Thr4- Thr, Met biosynthesis	+	+	+		
Glycolysis/related activities						
Q70CP7	Eno1-Enolase	+	+	+	+	+
P33284	Rag5-Hexokinase	+	+	+	+	+
Q6CNK3	Gpm1-Phosphoglycerate mutase	+	+	+	+	+
P17819	Tdh1-Glyceraldehyde-3-P dehydrogenase	+	+	+	+	+
Q6CX23	Tdh2-Glyceraldehyde-3-P dehydrogenase	+	+	+	+	+
P14828	Pgk1-Phosphoglycerate kinase	+	+	+	+	+
Q6CJG5	Tpi1-Triosephosphate isomerase	[a]	+	[a]		+
Q9C2U0	Fba1-Fructose-bisphosphate aldolase	+	+	+		+
Q6CLT7	Bdh1-NAD-dep 2 3-butanediol dehydr.	+	+	+	+	+
P20369	Adh1-Alcohol dehydrogenase	+	+	+	+	+
P49383	Adh2-Alcohol dehydrogenase 2	+	+		+	+
Q6CSK8	Ima2-Oligo-1,6-glucosidase		+	+	+	+
Q6CJQ7	Osm1-Fumarate reductase	+	+	+	+	
Q6CKA1	Idp1-Isocitrate dehydrogenase	+	+	+	+	
Q12629	Pdc1-Pyruvate decarboxylase	+	+			+
Q05079	Fbp1-Fructose-1,6-bisphosphatase	+	+		+	
Folding, stress response activities						
Q6CQZ9	Hsc82-Cytoplasmic chaperone Hsp90 family	+	+	+	+	+
Q6CWT6	Tsa1-Thioredoxin-peroxidase	+	+	+	+	+
Q6CR27	Sfa1-Glutathione-dep formaldehyde dehydr.	+	+	+		+
P40952	Kye1-Enoate reductase 1	+	+	+		+
Q6CJB0	Ahp1-Thiol-specific peroxiredoxin		+	+		
Other function						
Q6CQ22	Cofl-Cofilin	+	+	+	+	+
P17128	Act1-Actin	+	+	+	+	+
Q6CXT4	Tif1-ATP-dependent RNA helicase eIF4A	+	+	+	+	+
P13998	Ipp1-Inorganic pyrophosphatase	+	+	+	+	+
Q6CWA2	Acb1-Acyl-CoA-binding protein	+	+	+	+	
Q6CJ39	Rtc3-Restriction of telomere capping protein 3	+	+			+
Q6CWC1	Car2-L-ornithine transaminase		+	+	+	+
Q6CV73	Uba1-Ubiquitin activating enzyme		+	+	+	

[a] Identified by Wb.

2.6. Preparation of Rattus norvegicus RBC

Blood samples from *R. norvegicus* collected in EDTA were centrifuged and plasma was removed. The red cells were hemolysed in ice-cold 20 mM Tris–HCl, pH 7.5, 1 mM EDTA, 150 mM NaCl, 1% NP40 containing protease inhibitor cocktail (Complete, Roche) incubated 30 min on ice and then centrifuged (4 °C, 15,000 *g*, for 15 min) to remove ghosts and intact cells. The hemolysate was subjected to precipitation orderly with 45% and 65% ammonium sulfate.

Table 3
Proteins identified by nanoLC–ESI-MSMS in the G6PDH band from extract of *S. cerevisiae* glucose-grown culture, as compared to *K. lactis* data.

Protein, activity/pathway	*S. cerevisiae*	*K. lactis*
PPP/related activities		
Zwf1-Glucose 6-P dehydrogenase	+	+
Met6-Met, Cys, Thr, Sulfur pathway	+	+
Thr4-Thr, Met biosynthesis	+	+
Sah1-Met, Sulfur pathway	+	+
Ade17-His, purine/pyrimidine biosynth.	+	
Ade16-His, purine/pyrimidine biosynth.	+	
Ade1-His, purine/pyrimidine biosynth.	+	
Adk1-His, purine/pyrimidine biosynth.	+	
Shm2-Ser, Gly, purine/pyrimidine biosynth.	+	
Cys4-Cys, and sulfur aminoacids biosynth.	+	
Ade5,7-His, purine/pyrimidine biosynth.	+	
Ade6-Purine/pyrim. biosynth	+	
Glycolysis/related activities		
Eno1/Eno2-Enolase	+	+
Pgk1-Phosphoglycerate kinase	+	+
Hxk1/Hxk2-Hexokinase	+	+
Adh1-Alcohol dehydrogenase 1	+	+
Pdc1-Pyruvate decarboxylase	+	+
Fba1-Fructose-bisphosphate aldolase	+	+
Tdh3/Tdh2-Glyceraldehyde-3-P dehydr.	+	+
Pgi1-Glucose 6-P isomerase	+	+
Gpm1-Phosphoglycerate mutase 1	+	+
Tpi1-Triosephosphate isomerase	*	*
Folding, stress response activities		
Hsc82/Hsp82-Hsp90 family	+	+
Ssa1/Ssa2-Hsp70 family	+	+
Ssb1/Ssb2-Hsp70 family	+	+
Hsp12-Hsp12 family	+	+
Sse1-Hsp90 family	+	
Tsa1-Thioredoxin-peroxidase 1	+	+
Oye2-Old yellow enzyme	+	+
Sod1-Cu/Zn SOD	+	
Other function		
Act1-Actin	+	+
Cof1-Cofilin	+	+
Tif2-Translation initiation factor	+	+
Car2-Arg catabolism, ornitine biosynth.	+	+
Ipp1-Inorganic phosphatase	+	+
Gln4-Glutamine tRNA synthetase	+	+
Bmh1/ Bmh2-14-3-3 protein	+	

* Identified by Wb.

Most of the hemoglobin was observed to precipitate with 45% ammonium sulfate, whereas the G6PDH activity was measured in the 65% ammonium sulfate fraction. The enzyme solution was dialysed in 50 mM K-phosphate-50 mM K-acetate buffer (pH 7.0).

3. Results

3.1. G6PDH is a component of putative macromolecular proteins structures

Previously we showed by in-gel activity staining assays the presence of a single G6PDH band in extracts from *K. lactis* respiratory growth cultures (Fig. 1, lane 4), two bands when cells were grown in fermentative conditions or in the presence of ethanol (Fig. 1, lane 3) and many bands (lane 5) when the same strain was transformed with the plasmid containing the wild type *ZWF1* gene, coding for the G6PDH, fused to the GFP gene [17].

The slow-migrating native G6PDH band was called S for *S*uperior-migrating, while the faster migrating band was called I for *I*nferior-migrating. The appearance of the I G6PDH band is strictly correlated to the intracellular accumulation of NAD(P)H [17]. In contrast, when the *S. cerevisiae* cellular extracts were run and stained for G6PDH activity in native PAGE, they showed only one band, independently of growth conditions, (Fig. 1 lanes 1–2), with different migrating properties with respect to *K. lactis* G6PDH-specific bands [17]. When the S and I G6PDH bands were cut from native PAGE, eluted and fractioned on SDS-PAGE they showed, surprisingly, an almost identical pattern characterized by a number of proteins with different

Table 4
Proteins identified by nanoLC–ESI-MSMS in the Adh1 bands from extract of *K. lactis* and *S. cerevisiae* glucose-grown cultures.

Protein name	Activity	*K. lactis*	*S. cerevisiae*
K. l–S. c			
PPP and related activities			
Met6	**Met, Cys, Thr, sulfur pathway**	+	+
Gnd2	6-phosphogluconate dehydr.	+	+
Tal1	**Transaldolase**	+	
Tkl1	Transketolase	+	
Shb17	Sedoheptulose bisposph	+	
Ade17	**Purine/pyrim. biosynth**		+
Cys3	Cys biosynth.		+
Glycolysis and related activities			
Adh1	**Alcohol dehydr.**	+	+
Eno1–Eno2/Eno1	**Enolase**	+	+
Pgk1	**Phosphoglycerate kinase**	+	+
Tdh2–Tdh3/Tdh2	**Glyceraldehyde-3-P dehydr.**	+	+
Tdh1–Tdh1	**Glyceraldehyde-3-P dehydr.**	+	+
Gpm1	**Phosphoglycerate mutase**	+	+
Fba1	**Fructose-bisphosphate aldolase**	+	+
Rag5–Hxk2/Hxk1	**Hexokinase**	+	+
Ald4	Aldehyde dehydr.	+	+
Rag6–Pdc1	**Pyruvate decarboxylase**	+	+
Tpi1	**Triosephosphate isomerase**	*	+
Rag2–Pgi1	**Glucose-6-P isomerase**	+	+
Pgm1	Phosphoglucomutase	+	
Xyl1	Xylose reductase NAD(P)H-dep.	+	
Gcy1	Gycerol dehydrogenase	+	
Hor2	Glycerol-1 phosphatase		+
Folding, stress response activities			
Hsp12	**Hsp12 family**	+	+
Hsc82–Hsc82/Hsp82	**Hsp90 family**	+	+
Ssa2–Ssa2/ Ssa1	**Hsp70 family**	+	+
Ssb2–Ssb2/Ssb1	**Hsp70 family**	+	+
Ssa3–Ss3/Ssa4	Hsp70 family	+	+
Sse1	**Hsp70 family**	+	+
Tsa1	**Thioredoxin-peroxidase**	+	+
Kye2–Oye2	**Enoate reductase**	+	+
Ahp1	**Peroxiredoxin**	+	+
Hyr1	Glutathione peroxidase	+	
Grx1	Glutathione-dep. oxidoreduct	+	
Other function			
Cof1	**Cofilin**	+	+
Act1	**Actin**	+	
Asc1	Core component 40S rib	+	+
Bat1	Branched chain aa aminotransf.	+	
Tfs1	Carboxypeptidase Y inhibitor	+	
Gdh1	Glutamate dehydr.		+
Ymr226c	NADP-dep. Ser dehydr.		+
Ipp1	**Inorganic phosphatase**		+
Tif2	**Transl. initiation factor**		+

In bold components present in the G6PDH-containing complex.
* Identified by Wb.

molecular weight (MW) and intensity (Fig. 2A). This result suggests that the two G6PDH oligomers could be associated with other proteins or there could be a coincidental migration of these proteins with G6PDH on native gel.

In an attempt to separate the G6PDH-associated components, proteins extracted from the S G6PDH native band were fractionated by gel filtration. As reported in Fig. 2B, the collected fractions, analyzed for MW and G6PDH activity, showed three peaks: a high MW one (eluted in the void volume) containing low G6PDH activity (0.25 U)

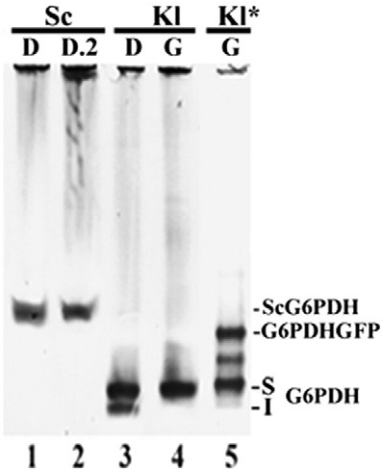

Fig. 1. In-gel native assays for G6PDH. G6PDH-stained activities separated on native PAGE. Cellular extracts were prepared from *S. cerevisiae* (Sc), *K. lactis* (Kl) and *K. lactis* expressing G6PDH/GFP (Kl*) cultures grown on 0.2% (D.2) and 2% glucose (D) and 2% glycerol (G).

and two other peaks with higher G6PDH activity (2.05 and 1.65 U, respectively) and MWs comprised between 403 and 261 kDa. However, the great number of bands obtained by separation on SDS-PAGE of proteins contained in peaks 2 and 3 (Fig. 2B lanes 2 and 3), similar to those of Fig. 2A lane 1, indicated that the MWs determined in the two fractions from gel filtration (403 and 261 kDa) cannot correspond to the combined total MW of all bands.

The most abundant proteins observed in SDS-PAGE were identified by MALDI-TOF analysis. These are G6PDH (→; MW = 56,574 Da), enolase (Eno1○; MW = 46,518 Da) and triosephosphate isomerase (Tpi1*; MW = 27,067 Da), in both bands (Fig. 2A). Moreover, the protein pattern observed in Fig. 2A is reproducible with little changes depending on carbon sources/growth conditions. In fact, the S and I G6PDH bands obtained from late exponential glucose-grown cells (Fig. 2C, lanes 1 and 2) or stationary glucose plus ethanol growth conditions (lanes 3 and 4), as well as the single S G6PDH-specific band from glycerol-grown cell extract (lane 5), showed on SDS-PAGE an almost identical pattern although with different but specific bands expressed at higher levels.

Finally, we analyzed mutant strains to test for the specific disappearance of some of the protein bands identified by MALDI-TOF analysis (Fig. 2A lane 1). The native S G6PDH bands purified from the glycolytic *Kleno1Δ*, *Kltpi1Δ* and *Klpgk1Δ* mutants, were analyzed by SDS-PAGE and western blot (Wb). The proteins patterns of the six strains showed the absence of Eno1 (○) (Fig. 3A lane 2), Tpi1 (*) (lane 4) and of the phosphoglycerokinase Pgk1 (>) (lane 6) proteins in the mutants, as compared to the parental strains (lanes 1, 3 and 5). The absence of Eno1, Tpi1, and Pgk1 from the G6PDH-specific band of the corresponding mutants was also confirmed by Wb using antibodies against Eno1, Tpi1 and Pgk1 (Fig. 3B lanes 2, 4 and 6 vs. lanes 1, 3 and 5) while, the G6PDH antibody was used to detect for the presence of the G6PDH activity (lanes 5 and 6).

3.2. Identification of the G6PDH-associated proteins by LC-MSMS

Protein components of S and I bands were identified by nanoLC–ESI-MSMS following proteolysis with two different peptidases (trypsin or chymotrypsin). We have shown that on native gel the recombinant G6PDH/GFP tagged fusion protein migrates differently from G6PDH (Fig. 1 lane 5 vs. lane 4). Therefore, to prove that the components of the S and I bands are truly associated with G6PDH and are not resulting from a coincidental migration on clear native PAGE, the proteins associated with the G6PDH/GFP band [17], obtained from

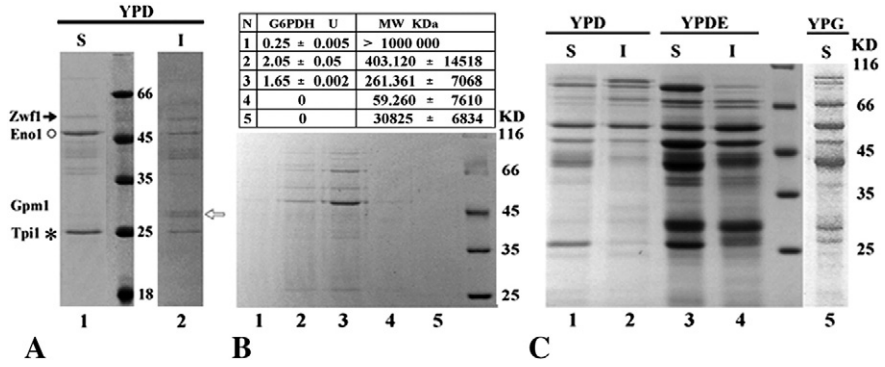

Fig. 2. The G6PDH is tightly associated with other proteins. (A–C) SDS-PAGE of G6PDH bands (S and I) eluted from native PAGE fractioned extracts. Cultures were grown on glucose (YPD), glucose + ethanol (YPDE) and glycerol (YPG). G6PDH (Zwf1), enolase (Eno1), triosephosphate isomerase (Tpi1) and glycerophosphomutase (Gpm1) activities were identified by MALDI-TOF analysis. (B). Gel filtration analysis of the S G6PDH band. G6PDH activity, MW and SDS-PAGE of harvested fractions were determined from glycerol-grown extract culture.

glycerol-grown cellular extracts, were also identified and compared with those of the lower migrating G6PDH band (Tables S4 and S5).

The analysis by nanoLC–MS/MS mass spectrometry of S and I G6PDH and G6PDH/GFP bands has generated a long list of shared proteins. All the proteins identified have been classified as mainly involved in PPP, in glycolytic/fermentative pathways, in folding and stress response, amino acids biosynthesis/degradation, cytoskeleton components or other processes (Table 2).

Unless the *K. lactis* protein name was previously assigned (e.g. Rag5), the name of each protein was reported on the basis of its highest identity to the corresponding *S. cerevisiae* ortholog protein. Tpi1, a protein present at high levels in the G6PDH bands, as suggested by MALDI-TOF, immunoblot and mutant analyses, was identified only following proteolysis with the chymotrypsin peptidase.

3.3. Identification of G6PDH-associated proteins in S. cerevisiae and R. norvegicus

To check if G6PDH is associated with other proteins also in bakery's yeast (Fig. 1 lanes 1–2), cellular extracts from *S. cerevisiae* were fractioned on native PAGE and stained for G6PDH activity. The activity band was cut, eluted and run on SDS-PAGE. As shown in Fig. 4A, the pattern obtained from *S. cerevisiae* G6PDH activity band (lane 2) resembles those of *K. lactis* (Fig. 2A), indeed, among the G6PDH-associated proteins, we were able to identify by Wb the enolase(s) and the Tpi1 proteins (Fig. 4A lane 4).

Proteins eluted from the G6PDH-specific band were analyzed by nanoLC–ESI-MSMS, following proteolysis with trypsin, to identify the proteins associated with G6PDH in *S. cerevisiae* (Table S6). As reported in Table 3, a large number of G6PDH-associated proteins are conserved in the two yeasts. In fact, all the glycolytic enzymes identified in *K. lactis* are also present in the G6PDH band from *S. cerevisiae*. In contrast, the major differences between the two yeasts concern enzymes involved in the synthesis of purine/pyrimidine (Table 2 vs. Table 3).

The identification of proteins associated with G6PDH also in higher eukaryotes might be a strong indication of the existence of an evolutionary conserved complex. Therefore, we analyzed the G6PDH activity

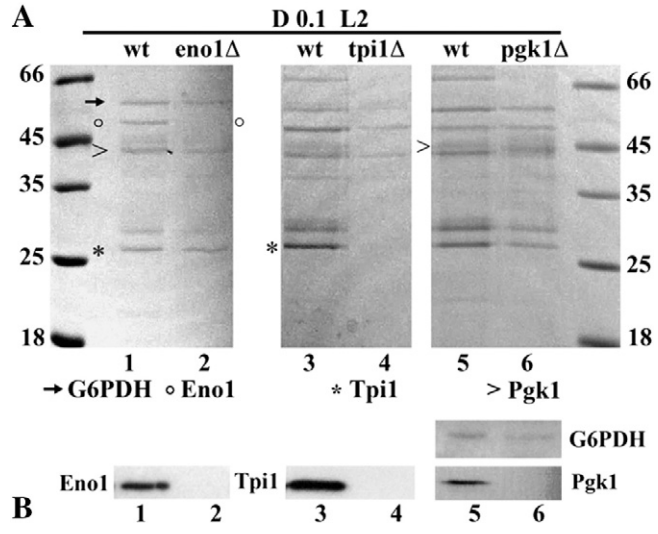

Fig. 3. The G6PDH complex contains glycolytic enzymes. (A) SDS-PAGE of S G6PDH-specific band from fractioned extracts of *Kleno1Δ*, *Kltpi1Δ* and *Klpgk1Δ* mutants and wild type strains cultures grown on rich 0.1% glucose + 2% lactate medium (D0.1 L2). (B) Wb of (A) using antibodies against Eno1, Tpi1, Pgk1 and G6PDH.

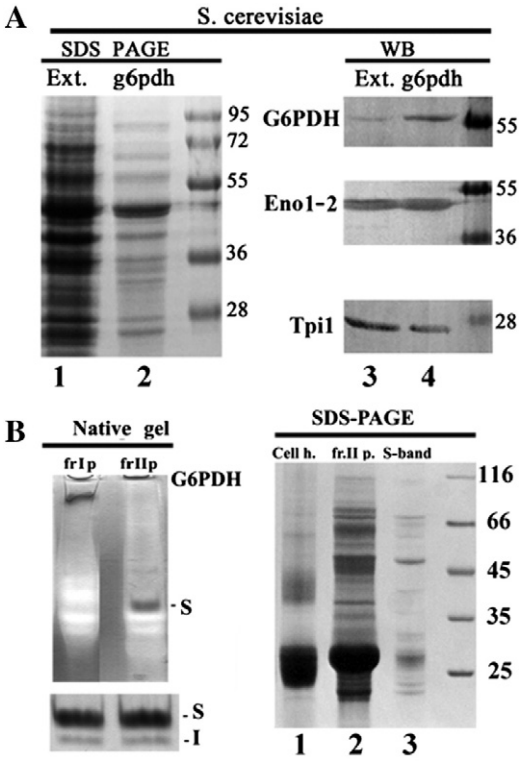

Fig. 4. (A) G6PDH-associated activities in *S. cerevisiae*. SDS-PAGE of the G6PDH native band and total extract (Ext.) prepared from glucose-grown cultures. Wb of lanes 1–2 using antibodies against Eno1, Tpi1 and G6PDH. (B) Native and SDS-PAGE of G6PDH from *Rattus norvegicus*. Upper panel: Native G6PDH staining of 45% (frIp) and 65% ammonium sulfate fractionated hemolysate (frIIp) from rat RBC. Lower panel: Native G6PDH staining of the frIIp. Right panel: SDS-PAGE of the S-band (lane 3), frIIp (lane 2) and RBC hemolysate (lane 1).

band from *R. norvegicus* erythrocytes, in which G6PDH deficiency could lead to severe enzymopathies [25]. To this end, we prepared red blood cell (RBC) hemolysate and identified, by in-gel staining assay, the G6PDH activity in the 65% ammonium sulfate fraction (Fig. 4B frIIp). The G6PDH S band was cut, eluted and purified (Fig. 4B lower panel) and an aliquot (Fig. 4B, lane 3) was analyzed and compared, by SDS-PAGE, to the 65% ammonium sulfate fraction (lane 2) and to the cellular hemolysate sample (lane 1). The proteins components of the S band were identified by nanoLC–ESI-MSMS, following proteolysis with trypsin (Table S7). The results showed high levels of RBC-specific proteins (hemoglobins, globins, carbonic anhydrases), the presence of fewer glycolytic enzymes, which are among the most abundant in yeasts G6PDH-specific bands, and NADPH-dependent proteins for reductive/stress response reactions.

3.4. Identification of Adh1-associated proteins in K. lactis and S. cerevisiae

The presence of ADHs among the G6PDH-associated proteins from both *K. lactis* (Adh1 and Adh2 in Table 2) and *S. cerevisiae* (Adh1 in Table 3) raised questions on their presence in these complexes. In *K. lactis* four *ADH* genes have been identified (*ADH1-4*). These genes are regulated at transcriptional level by carbon sources-dependent growth conditions [18]. The corresponding activities have been identified by genetic analysis in native PAGE by an ADH-specific staining assay [18,26]. The native ADH activities, obtained from extracts of glucose-, ethanol- or glycerol-grown cultures, show different migrating properties with respect to G6PDH (Fig. 5A, lanes 1–3). In Fig. 5A, we also reported the *adh* null strain pattern devoid of ADH activities (lane 4) [27] or harboring a re-integrated copy of *ADH1* in its chromosomal locus to confirm its migrating property on native PAGE (lane 5) [17]. As a control, the separated staining assays of G6PDH (lane 6) and ADH (lane 7) from the latter strain are also shown. The native assays for ADH and G6PDH activities from *S. cerevisiae* displayed similar results (Fig. 5B), where Adh1 is the fermentative activity involved in the production of ethanol during the growth on glucose (lanes 1–2) [28]. Adh2, not present on 2% glucose, is involved in the oxidation of the ethanol produced during fermentation (Fig. 5B lane 1) [29]. Adh3 is the mitochondrial component of the ethanol/acetaldehyde shuttle (Fig. 5B lane 2) [30], while Adh5 is responsible for the production of long chain fusel alcohols (lane 1) [31].

Since native ADH- and G6PDH-specific staining of *K. lactis* extracts showed different bands of activities well separated from each other, why have both Adh1 and Adh2 been identified in the G6PDH bands? (Table 2). To answer this question, the cellular extract prepared from the *K. lactis* strain expressing only Adh1 was fractionated on native PAGE and the S and I G6PDH- and Adh1-specific bands of activities recovered from this gel were analyzed by SDS-PAGE. Remarkably, also on denaturing gel the Adh1-specific band showed a complex protein pattern characterized by a number of different bands (Fig. 5C lane 1), slightly different from the G6PDH patterns (lanes 2 and 3). However, when the S and I G6PDH- and Adh1-specific bands were tested by Wb, the Eno1 and Tpi1 proteins were identified at high levels in the three samples, while the amount of the G6PDH in the Adh1 band was barely detectable (Fig. 5C). In parallel, SDS-PAGE analysis of the Adh1-specific band purified from *S. cerevisiae* extract showed a pattern similar to the one evidenced in the *K. lactis* Adh1 band (Fig. 5C lane 4 vs. lane 1).

To identify the proteins associated with Adh1 in the *K. lactis* strain expressing only this ADH or from the *S. cerevisiae* BY4741 strain, these bands of activity, eluted from native PAGE, were analyzed by the nanoLC–ESI-MSMS following proteolysis with trypsin (Tables S8 and S9).

Data comparison showed that most of the proteins identified in the Adh1-specific bands were common to both yeasts (Table 4). Many of the proteins present in the Adh1 bands were previously identified in the G6PDH-specific bands (Tables 2 and 3), although, given the fermentative role of Adh1, a greater number of glycolytic enzymes were identified in the Adh1-specific bands (Table 4).

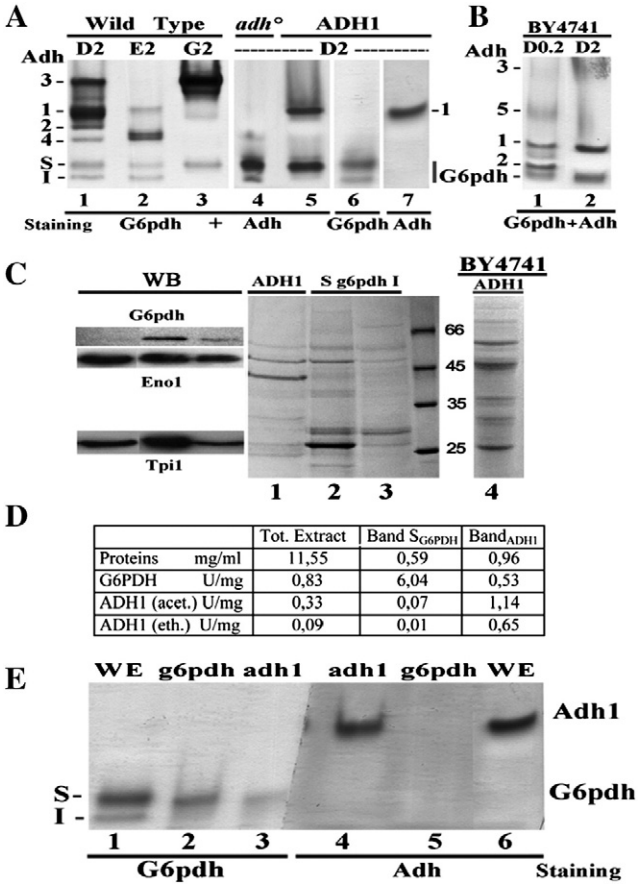

Fig. 5. Analyses of ADH and G6PDH complexes in *K. lactis* and *S. cerevisiae* protein extracts. (A) Native ADH and G6PDH isoforms in *K. lactis* and (B) *S. cerevisiae*. Cellular extracts were fractioned from the *K. lactis* CBS2359 strain, adh null (adh°) and adh° harboring a chromosomal reintegrated copy of *ADH1* (A, lanes 1–7) and *S. cerevisiae* BY4741 strain (B) cultures grown on 0.2 (D.2) and 2% glucose (D2), 2% ethanol (E2) and 2% glycerol (G2). On the left of lanes 1 are reported the migration of the Adh3, 1, 2, 4 and G6PDH S-I isoforms. (C) Wb and SDS-PAGE of Adh1 and G6PDH bands. Wb (Eno1, Tpi1 and G6PDH antibodies) of *K. lactis* eluted Adh1 and S - I G6PDH native bands from extracts of the adh° strain harboring a chromosomal copy of *ADH1* (lanes 1–3). SDS-PAGE of the *S. cerevisiae* Adh1 purified band (lanes 4). (D) Spectrophotometric determination of ADH and G6PDH. Activities were measured from total extract and Adh1-/S G6PDH-specific bands from the *K. lactis ADH1* strain culture of (A). The reported values are the averages of 3 independent experiments with a standard deviation of 6%–15%. (E) Native ADH- and G6PDH-specific refractioned bands. Staining assays of the eluted and refractioned S G6PDH- and Adh1-specific bands from the *K. lactis ADH1* strain. Total extract (WE) staining is reported as a control.

3.5. Different putative complexes contain common components

The presence of at least two different putative macromolecular structures containing a great number of identical proteins (see Tables 2, 3 and 4) raised the question as to whether these components were a) active in all complexes or b) kept in an active or in a reversible inactive state according to growth conditions in others.

To test the active state of these proteins the ADH and G6PDH activities were assayed in the whole extract of the *K. lactis ADH1* strain and in the eluted S G6PDH- and Adh1-specific bands. This analysis, as reported in Fig. 5D, showed 7 times more G6PDH activity in the eluted S G6PDH band, as compared to the whole extract (6.04 vs. 0.83 U/mg), but G6PDH activity was also present in the Adh1 band (0.53 U/mg). The presence of this enzymatic activity in the Adh1 band was further confirmed by its re-fractioning and staining for G6PDH on native PAGE (Fig. 5E lane 3).

The activity of Adh1 in the eluted bands and whole extract was measured in both directions i.e. giving as substrate either acetaldehyde and NADH (forward reaction) or ethanol and NAD^+ (reverse reaction). The results tabled in Fig. 5D showed that the activity in the whole extract (0.33 U/mg and 0.09 U/mg) and in the purified bands (1.14 U/mg and 0.65 U/mg) is higher with acetaldehyde and NADH than ethanol and NAD^+. Considering the forward reaction, measurement of the enzymatic activity showed an enrichment of 3.5 times in the Adh1 band as compared to the whole extract (1.14 vs. 0.33 U/mg). On the contrary, in the G6PDH band the ADH activity measured in the reverse direction was almost undetectable (0.01 U/mg), no Adh1 activity could be detected in the native staining assay (in which ethanol and NAD^+ were provided) (Fig. 5E lane 5) and the amount of ADH determined in the whole extract was too low (0.09 U/mg) as compared to the one determined in the forward reaction (0.33 U/mg). However when the assay was carried out in the forward direction the Adh1 activity in the G6PDH-specific band was detected (0.07 U/mg), confirming the presence of this enzyme among the components associated with G6PDH activity (Table 2). On the other hand, even though in the Adh1-specific band the G6PDH was detected by immunoblot analysis (Fig. 5C) and its activity was measured in both enzymatic assay and native staining (Fig. 5D and E lane 3), it was not identified between the components of the Adh1 band from native gel (Table 4).

3.6. $NAD(P)^+$/NAD(P)H balance affects components of metabolic alternative complexes

The different amounts of ADH activity determined in the forward and the reverse direction in the crude extract and in the Adh1 and G6PDH bands suggested a role of the $NAD(P)^+$/NAD(P)H ratio on the folding of ADH and G6PDH inside these complexes. Accordingly, a certain amount of Adh1 in the whole extract might be present in a reversible inactive state in other alternative complexes, like the G6PDH-specific one, and be activated by the addition of NADH excess but not NAD^+. Moreover, we have previously shown that the NAD^+(H)/$NADP^+$(H)-dependent cytosolic ADH and aldehyde dehydrogenase (Ald) balance affects the assembly of the G6PDH triggering an alteration in its oligomeric state, while NAD(P)H accumulation was directly responsible for the appearance of the G6PDH dimer activity [17]. Therefore, to test the role of the cofactors on the assembly and the stability of *K. lactis* ADH- and G6PDH-containing complexes, crude protein extracts were incubated in vitro in the presence of increasing concentrations of cofactors. The analysis has been performed in two different strains (CBS2359 and MW179-1D) to show that modifications of the ADH and G6PDH native patterns are not only cofactors- but also strain-dependent (Fig. 6 lanes 1–14). In fact, the stability and the oligomeric state of the G6PDH seems to be strictly dependent on the concentrations of the NAD^+ and $NADP^+$ cofactors (Fig. 6 lanes 10–14), while no modification of the G6PDH was observed in the presence of increasing concentrations of the reduced cofactors in both CBS2359 (expressing two activity bands) and MW179-1D (showing only one band) (Fig. 6 lanes 1–9). In contrast, while the ADHs patterns were only slightly modified by the addition of NADPH (Fig. 6 lanes 6–9), they showed to be affected by both NAD^+ and $NADP^+$ (lanes 10–14). Interesting results were obtained incubating the extracts with NADH, a cofactor that feeds, during the growth on glucose, the glycolytic flux due to its cycled reoxidation by fermentative ADHs. In fact, Adh1 and Adh2 were greatly increased in the presence of growing concentrations of NADH (Fig. 6 lanes 1–5) and at higher levels in the MW179-1D strain, as compared to the CBS2359 strain (Fig. 6A lanes 1–5). In addition, the increased levels of the Adh1 and Adh2 activities (Fig. 6 lanes 1–5) could also explain the higher quantity of ADH assayed on the whole extract and in the G6PDH band, giving acetaldehyde and NADH as substrate, as compared to the activity determined on the purified Adh1 band (Fig. 5D).

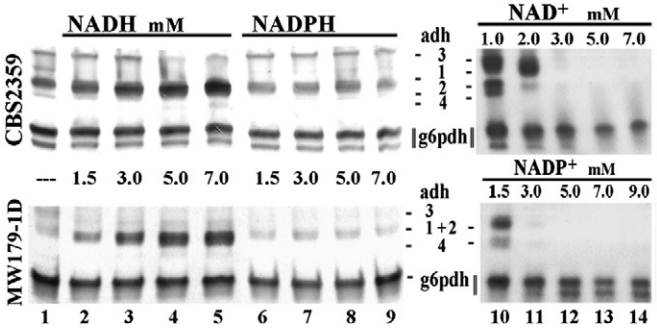

Fig. 6. Effects of $NAD(P)^+$ and NAD(P)H on the ADH and G6PDH complexes. ADH and G6PDH native-gel stained activities following in vitro-incubation of extracts with increasing concentration of NAD(P)H and $NAD(P)^+$. The extracts (about 10 μg/lane), prepared from MW179-1D and CBS2359 cultures grown on YPD, were incubated over night on ice with the cofactors and fractioned on native PAGE.

3.7. Native assays for Pgi, Hxk and Ald activities suggested their presence in different complexes

To test the active state of other glycolytic enzymes identified in the Adh1-, S and I G6PDH-specific complexes (Tables 2 and 4), staining assays for phosphoglucose isomerase (PGI) and hexokinase (HXK) activities were carried out in parallel with ADH and G6PDH stained activities on native PAGE.

Staining for Pgi, tested on extracts from different carbon sources-grown cultures, showed a unique band of activity migrating on native PAGE, neither at the level of the Adh1 nor of the G6PDH bands but roughly at the level of Adh4 (Fig. 7A lanes 1–4 vs. 5–8). In parallel, in-gel staining Hxk assay showed bands of activities with different carbon sources-dependent migrating properties (Fig. 7A lanes 10–13). Moreover, major Hxk bands seemed to migrate with the S and I G6PDH-specific bands (Fig. 7A lanes 5–7 and 9). This is in line with mass spectrometry analysis of the G6PDH-specific bands, which contain Hxk (Tables 2 and 3). The absence of a Hxk migrating band, similar to Pgi, at the level of the Adh1 indicated that these enzymes could be inactive in this complex.

Finally, we also tried to identify, by staining assays, the migrating properties of aldehyde dehydrogenase (ALD) activities. Five different *ALD* genes have been identified in the genome of *K. lactis* [32]. Although these genes have not been characterized, sequences comparison suggested that they might code for the putative Ald2, Ald3, Ald4, Ald5 and Ald6 *S. cerevisiae* orthologs which require either magnesium or potassium for their catalytic activity and have different affinities for either NAD^+ and/or $NADP^+$ [33]. In-gel Ald staining assays, providing potassium and NAD^+ in the staining mixture, showed the presence of different carbon sources-dependent bands of activities (Fig. 7B lanes 6–10) with migrating properties identical, to those of the ADH, with the exception of the slower migrating band (lanes 1–4). Also this evidence agrees with mass spectrometry analysis, being the Ald4 protein present in Adh1-specific band (Tables 4 and S8). On the contrary, $NADP^+$/magnesium-dependent Ald activities showed two native bands (Fig. 7B lanes 12–14), probably identical to the slower migrating bands previously identified with NAD^+ as cofactor (lanes 7–10). Notably, one of these two bands migrates at the level of Adh3 (Fig. 7B lanes 2–3), while the other one disappears when the cells were grown in the presence of antimycin A (lanes 6 and 11), an inhibitor of the electron transport chain. The mutant strain devoid of the only gene coding for pyruvate decarboxylase (Rag6/Pdc1), therefore unable to accumulate acetaldehyde, only displayed the slower migrating band in both Ald assays (Fig. 7B lanes 10 and 14).

To test whether all the different stained activities could be localized more precisely on native PAGE, extracts prepared from wild type and mutant strains from different carbon sources-grown conditions were fractioned in parallel in two native gels. One of these gels was first

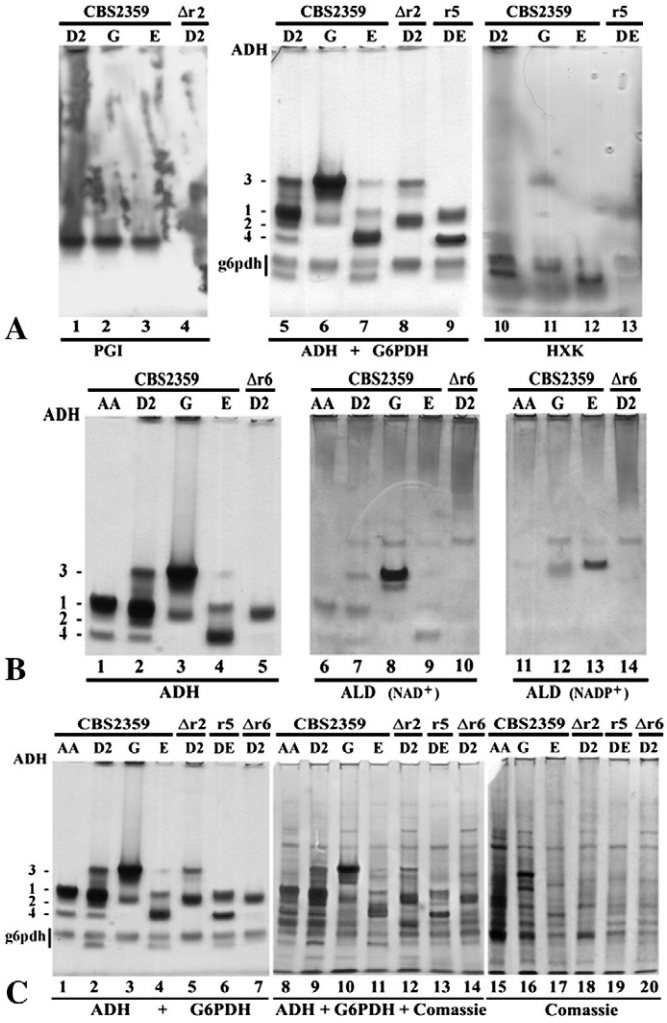

Fig. 7. (ABC) In-gel native assays for PGI, HXK, ALD ADH, ALD, G6PDH activities and Coomassie. (A) Parallel in-gel native comparison between PGI–HKX and ADH–G6PDH stained activities. (B) Comparison between native ALD and ADH stained activities. (C) Native gel was first stained for ADH and G6PDH activities and then for Coomassie and compared with a native Coomassie-stained gel. The extracts were prepared from the CBS2359 and *rag2*Δ (Δr2), *rag5* (r5) and *rag6*Δ (Δr6) mutant strains cultures grown on 5% glucose + antimycin A (AA), 2% glucose (D2), 2% glycerol (G), 2% ethanol (E) and 1% glucose + 1% ethanol (DE).

assayed for ADH and G6PDH activities (Fig. 7C lanes 1–7) followed by Coomassie staining (lanes 8–14) while the second one was directly stained with Coomassie (lanes 15–20). This experiment allowed, by direct comparison of the distinct bands on the two gels, the localization of each activity within a precise and discrete Coomassie band whose intensity varied according to growth conditions and mutant strains (Fig. 7C lanes 1–20).

4. Discussion

In gel-activity staining assay allows the visualization of different active oligomeric states of enzymes (e.g. G6PDH) and to distinguish between activities (e.g. ADH) coded by two or more genes [18]. Previously, we demonstrated that the two *K. lactis* G6PDH-specific activities represent different oligomeric state of the enzyme determined by the cytosolic ratio between the NADH-dependent fermentative Adh1 and the NADPH-dependent Ald6 pyruvate dehydrogenase bypass [17]. In fact, cytosolic equilibrium of the two reduced cofactors, in physiological conditions, is determined by the cell requirement for energy (ATP), biomass synthesis and stress response [17]. During the characterization of the two G6PDH isoforms, we found, by SDS-PAGE analysis of the purified bands, a great number of proteins associated with G6PDH in both *K. lactis* (Figs. 2 and 3) and *S. cerevisiae* yeasts (Fig. 4).

Immunoprecipitation techniques using antibodies against G6PDH or GFP (in strains expressing G6PDH/GFP) or against Eno1 and Tpi1 proteins (identified by MALDI-TOF analysis in the G6PDH bands; Figs. 3 and 4), did not allow the isolation of proteins from neither crude extract nor from the eluted G6PDH bands (data not shown). Conversely, gel filtration (Fig. 2B) resulted unable to solve single components suggesting a tight association of these proteins to G6PDH.

The components of the purified G6PDH-specific bands from *K. lactis* and *S. cerevisiae* were identified by nanoLC–ESI–MS/MS mass spectrometry following proteolysis with two different peptidases (Tables 2, 3 and S1–S6) and were classified into three major groups: glycolytic/fermentative enzymes, PPP enzymes that use its intermediates for the synthesis of pyrimidines/purines, cofactors or sulfur-containing aminoacids (Fig. S1) and proteins required for folding and response to stress. Remarkably, most of the proteins identified in the *K. lactis* G6PDH bands are also present in the *S. cerevisiae* G6PDH band (Table 3) despite the different migrating properties (Fig. 1). Moreover, glycolytic (enolase, triosephosphate isomerase and phosphoglycerate mutase) and GSH-dependent proteins were identified in the G6PDH-specific band from rat erytrocytes (Table S7), confirming the presence of this macromolecular structure also in RBC [34]. In fact, differently from the G6PDH of yeasts, in RBC (a mammalian cell devoid of mitochondria and mainly devoted to the transport of oxygen and CO_2) the primary role of this activity is to provide readily available NADPH. This cofactor in RBC is essential for the glutathione S-transferase, glutaredoxin- and thioredoxin-dependent cell neutralization systems. Indeed, as can be seen in Table S7, a large number of the proteins identified with the G6PDH band (GSH-dependent proteins, peroxiredoxin, SOD, Hsp proteins) require NADPH to regenerate their detoxification role [25].

Surprisingly, the G6PDH-specific band contains the Adh1 enzyme, whose activity can be assayed in native PAGE in a distant migrating position (Fig. 5A and B). Moreover, protein extracts did not display a continuous distribution on native PAGE Coomassie-stained gel but localize in discrete bands (Fig. 7) suggesting the intracellular organization of soluble proteins in macro-molecular network structures. The identification, by nanoLC–ESI-MS/MS mass spectrometry, of components associated with the *K. lactis* and *S. cerevisiae* Adh1-specific bands (Tables 4 and S8-S9) (Fig. S2) in common with the G6PDH bands (Fig. S1) (Tables 2 and 3) could be a strong indication of the existence of these macro-structures.

The presence of actin and cofilin, among the proteins identified in the G6PDH and Adh1 bands (Tables 2, 3 and 4), suggested a role for the cytoskeleton in the assembly/disassembly of these complexes. In *S. cerevisiae* actin filaments specifically interact with glycolytic enzymes (Hxk, Pgi, Ald, Tpi, Tdh, Pgk and Eno) constituting a multi-enzyme complex that increases the rate of ethanol production [35]. Moreover, G6PDH- and Adh1-specific bands contain high levels of molecular chaperones (Tables 2, 3 and 4) reported to be involved in the earlier folding stages and stabilization of protein complexes [36,37]. Indeed, chaperones and cochaperones have been found associated with the purinosome complex where the Hsp90/Hsp70-based machinery is implicated in its assembly [36]. These proteins could have a similar role in the formation of the G6PDH- and ADH-containing complexes. Finally, it must be pointed out that many components of the two complexes were already reported as associated with G6PDH and Adh1 in the *S. cerevisiae* database of interactions (String database for known and predicted protein–protein interactions; http://string-db.org/).

On the contrary, the diverse *S. cerevisiae* and *K. lactis* niches could account at the same time for: a) the distinctive expression of the oxidative part of the PPP, Hsp activities and enzymes for the synthesis of purines/pyrimidines in the two yeasts [38] (Figs. S1 and S2) and: b) the different components in the G6PDH- and Adh1-containing complexes (Table 3).

The *K. lactis* and *S. cerevisiae* G6PDH- and Adh1-containing complexes are large macromolecular structures in which not all the components are active. This was demonstrated comparing, by in-gel staining assays, the Pgi, the Hxk, and the Ald activities with ADH and G6PDH (Fig. 6ABC), key enzymes located at major metabolic cross-routes between glycolysis (Hxk1) or gluconeogenesis and PPP (Pgi1), pyruvate dehydrogenase bypass (Ald), fermentation or alcohol respiration (ADH) (Figs. S1 and S2). We observed that Pgi1, which was identified in the Adh1 band (Table 4), is active at the level of Adh4 (Fig. 7A lanes 1–4). Moreover, Hxk activity (*RAG5* is the unique *K. lactis HXK* gene,) was localized in different migrating bands (Fig. 7A lanes10–13) at the levels of the G6PDH oligomers (lanes 5–7), even though this protein was found associated with both G6PDH and Adh1 bands (Tables 2 and 4). The observed transition of the Hxk bands (Fig. 7A lanes 10–12) seems to be similar to those of the G6PDH isoforms [17] suggesting a common mechanism of regulation of the two activities inside the two complexes (see Fig. 8). Since acetaldehyde is a substrate required in many metabolic routes, Ald staining assays revealed multiple bands of activity at the levels of the ADHs (Fig. 7B lanes 1–14). This is in line with mass spectrometry analysis, because Ald4 was found associated with the Adh1 band (Table 4), and also with the mitochondrial Adh4 and Adh3 eluted bands (data not shown, manuscript in preparation).

All these data have demonstrated that several proteins involved in metabolism and response to stress are organized in dynamic intracellular complexes. These organizations could provide several advantages with regard to function and also to stability of single components, as reported for the fatty acid synthase (FAS) I system, a large coordinated multifunctional enzyme which carries out fatty acids biosynthesis [2]. This complex is specifically required during the transition from the respiratory to the fermentative growth constituting an evolutionary-conserved membrane-phospholipids adaptive system able to contrast the potential denaturing conditions determined by the accumulation of ethanol. Indeed, as previously reported, fermentative *K. lactis* mutants unable to accumulate ethanol and intracellular glycerol necessary to maintain redox balance show severe pleiotropic defects leading to altered lipid homeostasis with highly reduced *FAS1*/*FAS2* expression [39–41] and a slightly altered Coomassie-stained pattern in native gel (Fig. 7C lanes of Δr2, r5 Δr6 vs. CBS2359).

The comparison of G6PDH-containing complexes present in cellular extracts from *K. lactis* cultures has shown that the activities inside these complexes are dynamically lit and turned off according to nutrients, growth conditions and stress response (Fig. 7). In fact, as previously shown, the accumulation of the faster migrating I-G6PDH band occurs when the cytosolic $NAD(P)^+$/NAD(P)H reoxidation rate mainly operated by the mitochondrial Nde1 and Nde2 transdehydrogenases is limiting due to an altered balance between respiration and/or fermentation [17]. Since the proteins associated with the S and I bands are very similar (Table S1–S3) and the I migrating complex seems to be present all the time, as shown by Fig. 7C lanes 8–20, therefore, the migration of a portion of the S-associated proteins to the I band is determined by cytosolic NAD(P)H accumulation which leads to the reversible formation of a partial inactive depot. Conversely, the S band-associated proteins from glucose extracts are only slightly different as compared to those of glycerol. In fact, as shown in Table S1–S2 vs. S4–S5, the differences concern a slightly higher number of dehydrogenases, and of proteins required for the synthesis of purine/NAD^+, gluconeogenesis

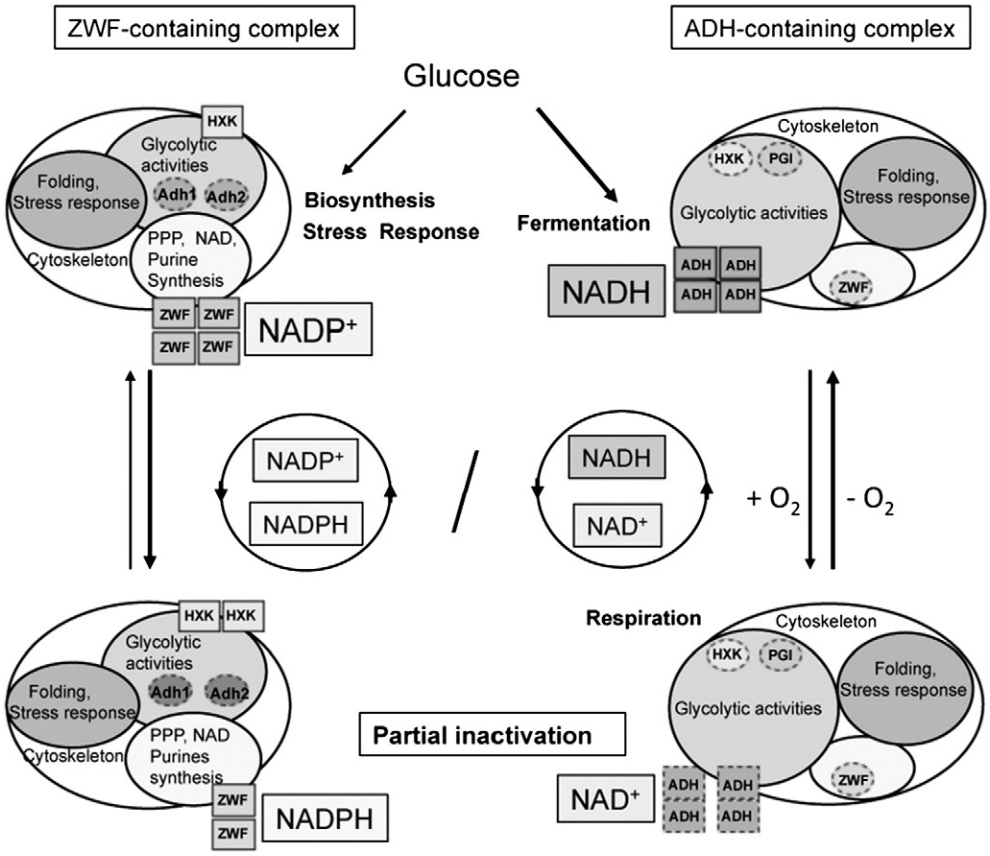

Fig. 8. Growth-transition model of the G6PDH- and Adh1-containing depots. Model showing how the $NAD(P)^+$/NAD(P)H redox balance ratio affects the equilibrium of the G6PDH- and Adh1-containing complexes during the growth on glucose. In the model we also suggested a role of oxygen on the control of the Adh1 complex but also on the G6PDH one during the growth-transition from respiratory to fermentative conditions. Square symbols indicate functional-, while circle inactive-activities.

(Ima2, β-glucosidase, Fbp1, Glc3) and for the oxidation of respiration carbon sources. These results further confirmed the fine physiological adaptive role of these complexes.

4.1. Conclusions

In-gel staining assays allowed the identification of several different activities (Fig. 7ABC), belonging to multi-components depots and, as previously suggested [3,42], we have shown that not all the components are active in a complex, but each component can be active/inactive or released/re-assorted inside these depots according to metabolic/pathological conditions. Moreover, the $NAD(P)^+$/NAD(P)H redox balance seems to affects the G6PDH and ADH activities [17] (Fig. 6C lanes 1–7). In fact, the in vivo changes of G6PDH- and ADH-specific activities during the physiological growth under different carbon sources (Fig. 5) or following the in vitro-incubation of crude extract with $NAD(P)^+$-NAD(P)H (Fig. 6), further confirmed that cofactors redox balance is one of the major factors affecting the different metabolic complexes (Fig. 7C lanes 15–20). A model which suggests that the role of the $NAD(P)^+$/NAD(P)H redox balance on the dynamic re-assortment/post-translational allosteric modulation of some of the components of the S and I G6PDH and Adh1 "depots" is reported in Fig. 8. We propose the cofactors reoxidation rate, influenced by nutrients availability, oxygen concentrations, environmental stresses, etc., as the mechanism tuning the dynamic adaptive equilibrium between the assembled metabolic depots.

Further investigations will help to analyze the assembly of protein complexes during physiological as compared to environmental stress or nutrient starvation conditions and/or during the progression through the cell cycle and the genetic control behind them. The development of in gel-native specific assays for activities involved in these pathways will allow the identification of functional components and of the corresponding putative intracellular depots in wild type and mutant strains.

Transparency document

The Transparency document associated with this article can be found, in the online version.

Acknowledgments

This work was funded by "Ateneo 2012" — Sapienza University of Rome (Prot. n. C26A112XHR). We would like to thank D. De Biase and C. Falcone for the support during the execution of this project. We would also like to thank C. Compagno, A. Fournier, P. Goffrini and M. Wesolowski-Louvel for the *tpi1*, *pgk1*, *rag5* and *eno1 K. lactis* mutants. G. Bruscalupi for the generosity in providing the RBC of *R. norvegicus*, C. Lanini for technical assistance, S. Cialfi for the help during the preparation of the RBC hemolysate and A. Giorgi for MALDI-TOFF analysis and for critical reading of the manuscript.

Appendix A. Supplementary data

Supplementary data to this article can be found online at http://dx.doi.org/10.1016/j.bbagen.2015.01.021.

References

[1] B. Alberts, The cell as a collection of protein machines: preparing the next generation of molecular biologists, Cell 92 (1998) 291–294.
[2] T. Maier, M. Leibundgut, D. Boehringer, N. Ban, Structure and function of eukaryotic fatty acid synthases, Q. Rev. Biophys. 43 (2010) 373–422.
[3] P.S. Ray, A. Arif, P.L. Fox, Macromolecular complexes as depots for releasable regulatory proteins, Trends Biochem. Sci. 32 (2007) 158–164.
[4] J. Wang, X. Peng, W. Peng, F.X. Wu, Dynamic protein interaction network construction and applications, Proteomics 14 (2014) 338–352.
[5] S.M. Eswarappa, P.L. Fox, Citric acid cycle and the origin of MARS, Trends Biochem. Sci. 38 (2013) 222–228.
[6] H. Zhao, J.B. French, Y. Fang, S.J. Benkovic, The purinosome, a multi-protein complex involved in the de novo biosynthesis of purines in humans, Chem. Commun. (Camb.) 49 (2013) 4444–4452.
[7] R.B. Bhavsar, L.N. Makley, P.A. Tsonis, The other lives of ribosomal proteins, Hum. Genom. 4 (2010) 327–344.
[8] A.C. Gavin, P. Aloy, P. Grandi, R. Krause, M. Boesche, M. Marzioch, C. Rau, L.J. Jensen, S. Bastuck, B. Dumpelfeld, A. Edelmann, M.A. Heurtier, V. Hoffman, C. Hoefert, K. Klein, M. Hudak, A.M. Michon, M. Schelder, M. Schirle, M. Remor, T. Rudi, S. Hooper, A. Bauer, T. Bouwmeester, G. Casari, G. Drewes, G. Neubauer, J.M. Rick, B. Kuster, P. Bork, R.B. Russell, G. Superti-Furga, Proteome survey reveals modularity of the yeast cell machinery, Nature 440 (2006) 631–636.
[9] N.J. Krogan, G. Cagney, H. Yu, G. Zhong, X. Guo, A. Ignatchenko, J. Li, S. Pu, N. Datta, A.P. Tikuisis, T. Punna, J.M. Peregrin-Alvarez, M. Shales, X. Zhang, M. Davey, M.D. Robinson, A. Paccanaro, J.E. Bray, A. Sheung, B. Beattie, D.P. Richards, V. Canadien, A. Lalev, F. Mena, P. Wong, A. Starostine, M.M. Canete, J. Vlasblom, S. Wu, C. Orsi, S.R. Collins, S. Chandran, R. Haw, J.J. Rilstone, K. Gandi, N.J. Thompson, G. Musso, P. St Onge, S. Ghanny, M.H. Lam, G. Butland, A.M. Altaf-Ul, S. Kanaya, A. Shilatifard, E. O'Shea, J.S. Weissman, C.J. Ingles, T.R. Hughes, J. Parkinson, M. Gerstein, S.J. Wodak, A. Emili, J.F. Greenblatt, Global landscape of protein complexes in the yeast *Saccharomyces cerevisiae*, Nature 440 (2006) 637–643.
[10] U. de Lichtenberg, L.J. Jensen, S. Brunak, P. Bork, Dynamic complex formation during the yeast cell cycle, Science (New York, N.Y.) 307 (2005) 724–727.
[11] J.D. O'Connell, A. Zhao, A.D. Ellington, E.M. Marcotte, Dynamic reorganization of metabolic enzymes into intracellular bodies, Annu. Rev. Cell Dev. Biol. 28 (2012) 89–111.
[12] A.G. Ngounou Wetie, I. Sokolowska, A.G. Woods, U. Roy, J.A. Loo, C.C. Darie, Investigation of stable and transient protein–protein interactions: past, present, and future, Proteomics 13 (2013) 538–557.
[13] S.W. Au, C.E. Naylor, S. Gover, L. Vandeputte-Rutten, D.A. Scopes, P.J. Mason, L. Luzzatto, V.M. Lam, M.J. Adams, Solution of the structure of tetrameric human glucose 6-phosphate dehydrogenase by molecular replacement, Acta Crystallogr. 55 (1999) 826–834.
[14] R. Notaro, A. Afolayan, L. Luzzatto, Human mutations in glucose 6-phosphate dehydrogenase reflect evolutionary history, FASEB J. 14 (2000) 485–494.
[15] R.F. Kletzien, P.K. Harris, L.A. Foellmi, Glucose-6-phosphate dehydrogenase: a "housekeeping" enzyme subject to tissue-specific regulation by hormones, nutrients, and oxidant stress, FASEB J. 8 (1994) 174–181.
[16] M. Saliola, G. Scappucci, I. De Maria, T. Lodi, P. Mancini, C. Falcone, Deletion of the glucose-6-phosphate dehydrogenase gene KlZWF1 affects both fermentative and respiratory metabolism in Kluyveromyces lactis, Eukaryot. Cell 6 (2007) 19–27.
[17] M. Saliola, A. Tramonti, C. Lanini, S. Cialfi, D. De Biase, C. Falcone, Intracellular NADPH levels affect the oligomeric state of the glucose 6-phosphate dehydrogenase, Eukaryot. Cell 11 (2012) 1503–1511.
[18] M. Saliola, C. Falcone, Two mitochondrial alcohol dehydrogenase activities of Kluyveromyces lactis are differently expressed during respiration and fermentation, Mol. Gen. Genet. 249 (1995) 665–672.
[19] M. Lemaire, M. Wesolowski-Louvel, Enolase and glycolytic flux play a role in the regulation of the glucose permease gene RAG1 of *Kluyveromyces lactis*, Genetics 168 (2004) 723–731.
[20] C. Donnini, F. Farina, B. Neglia, M.C. Compagno, D. Uccelletti, P. Goffrini, C. Palleschi, Improved production of heterologous proteins by a glucose repression-defective mutant of *Kluyveromyces lactis*, Appl. Environ. Microbiol. 70 (2004) 2632–2638.
[21] M.M. Bianchi, L. Tizzani, M. Destruelle, L. Frontali, M. Wesolowski-Louvel, The 'petite-negative' yeast Kluyveromyces lactis has a single gene expressing pyruvate decarboxylase activity, Mol. Microbiol. 19 (1996) 27–36.
[22] C. Compagno, F. Boschi, A. Daleffe, D. Porro, B.M. Ranzi, Isolation, nucleotide sequence, and physiological relevance of the gene encoding triose phosphate isomerase from *Kluyveromyces lactis*, Appl. Environ. Microbiol. 65 (1999) 4216–4219.
[23] A. Fournier, R. Fleer, P. Yeh, J.F. Mayaux, The primary structure of the 3-phosphoglycerate kinase (PGK) gene from *Kluyveromyces lactis*, Nucleic Acids Res. 18 (1990) 365.
[24] Y. Ishihama, Y. Oda, T. Tabata, T. Sato, T. Nagasu, J. Rappsilber, M. Mann, Exponentially modified protein abundance index (emPAI) for estimation of absolute protein amount in proteomics by the number of sequenced peptides per protein, Mol. Cell. Proteomics 4 (2005) 1265–1272.
[25] E. Beutler, G6PD deficiency, Blood 84 (1994) 3613–3636.
[26] C. Mazzoni, M. Saliola, C. Falcone, Ethanol-induced and glucose-insensitive alcohol dehydrogenase activity in the yeast Kluyveromyces lactis, Mol. Microbiol. 6 (1992) 2279–2286.
[27] M. Saliola, S. Bellardi, I. Marta, C. Falcone, Glucose metabolism and ethanol production in adh multiple and null mutants of *Kluyveromyces lactis*, Yeast 10 (1994) 1133–1140.
[28] U. Lutstorf, R. Megnet, Multiple forms of alcohol dehydrogenase in Saccharomyces cerevisiae. I. Physiological control of ADH-2 and properties of ADH-2 and ADH-4, Arch. Biochem. Biophys. 126 (1968) 933–944.
[29] C.L. Denis, M. Ciriacy, E.T. Young, A positive regulatory gene is required for accumulation of the functional messenger RNA for the glucose-repressible alcohol dehydrogenase from *Saccharomyces cerevisiae*, J. Mol. Biol. 148 (1981) 355–368.
[30] B.M. Bakker, C. Bro, P. Kotter, M.A. Luttik, J.P. van Dijken, J.T. Pronk, The mitochondrial alcohol dehydrogenase Adh3p is involved in a redox shuttle in *Saccharomyces cerevisiae*, J. Bacteriol. 182 (2000) 4730–4737.
[31] J.R. Dickinson, L.E. Salgado, M.J. Hewlins, The catabolism of amino acids to long chain and complex alcohols in Saccharomyces cerevisiae, J. Biol. Chem. 278 (2003) 8028–8034.

[32] B. Dujon, D. Sherman, G. Fischer, P. Durrens, S. Casaregola, I. Lafontaine, J. De Montigny, C. Marck, C. Neuveglise, E. Talla, N. Goffard, L. Frangeul, M. Aigle, V. Anthouard, A. Babour, V. Barbe, S. Barnay, S. Blanchin, J.M. Beckerich, E. Beyne, C. Bleykasten, A. Boisrame, J. Boyer, L. Cattolico, F. Confanioleri, A. De Daruvar, L. Despons, E. Fabre, C. Fairhead, H. Ferry-Dumazet, A. Groppi, F. Hantraye, C. Hennequin, N. Jauniaux, P. Joyet, R. Kachouri, A. Kerrest, R. Koszul, M. Lemaire, I. Lesur, L. Ma, H. Muller, J.M. Nicaud, M. Nikolski, S. Oztas, O. Ozier-Kalogeropoulos, S. Pellenz, S. Potier, G.F. Richard, M.L. Straub, A. Suleau, D. Swennen, F. Tekaia, M. Wesolowski-Louvel, E. Westhof, B. Wirth, M. Zeniou-Meyer, I. Zivanovic, M. Bolotin-Fukuhara, A. Thierry, C. Bouchier, B. Caudron, C. Scarpelli, C. Gaillardin, J. Weissenbach, P. Wincker, J.L. Souciet, Genome evolution in yeasts, Nature 430 (2004) 35–44.

[33] F. Saint-Prix, L. Bonquist, S. Dequin, Functional analysis of the ALD gene family of Saccharomyces cerevisiae during anaerobic growth on glucose: the NADP+-dependent Ald6p and Ald5p isoforms play a major role in acetate formation, Microbiology 150 (2004) 2209–2220.

[34] M.E. Campanella, H. Chu, P.S. Low, Assembly and regulation of a glycolytic enzyme complex on the human erythrocyte membrane, Proc. Natl. Acad. Sci. U. S. A. 102 (2005) 2402–2407.

[35] D. Araiza-Olivera, N. Chiquete-Felix, M. Rosas-Lemus, J.G. Sampedro, A. Pena, A. Mujica, S. Uribe-Carvajal, A glycolytic metabolon in Saccharomyces cerevisiae is stabilized by F-actin, FEBS J. 280 (2013) 3887–3905.

[36] J.B. French, H. Zhao, S. An, S. Niessen, Y. Deng, B.F. Cravatt, S.J. Benkovic, Hsp70/Hsp90 chaperone machinery is involved in the assembly of the purinosome, Proc. Natl. Acad. Sci. U. S. A. 110 (2013) 2528–2533.

[37] T. Makhnevych, W.A. Houry, The role of Hsp90 in protein complex assembly, Biochim. Biophys. Acta 1823 (2012) 674–682.

[38] R. Rodicio, J.J. Heinisch, Yeast on the milky way: genetics, physiology and biotechnology of Kluyveromyces lactis, Yeast 30 (2013) 165–177.

[39] S. Cialfi, D. Uccelletti, A. Carducci, M. Wesolowski-Louvel, P. Mancini, H.J. Heipieper, M. Saliola, KlHsl1 is a component of glycerol response pathways in the milk yeast *Kluyveromyces lactis*, Microbiology 157 (2011) 1509–1518.

[40] D. Gorietti, E. Zanni, C. Palleschi, M. Delfini, D. Uccelletti, M. Saliola, A. Miccheli, Depletion of casein kinase I leads to a NAD(P)(+)/NAD(P)H balance-dependent metabolic adaptation as determined by NMR spectroscopy-metabolomic profile in *Kluyveromyces lactis*, Biochim. Biophys. Acta 1840 (2014) 556–564.

[41] H.J. Heipieper, S. Isken, M. Saliola, Ethanol tolerance and membrane fatty acid adaptation in adh multiple and null mutants of Kluyveromyces lactis, Res. Microbiol. 151 (2000) 777–784.

[42] R. Narayanaswamy, M. Levy, M. Tsechansky, G.M. Stovall, J.D. O'Connell, J. Mirrielees, A.D. Ellington, E.M. Marcotte, Widespread reorganization of metabolic enzymes into reversible assemblies upon nutrient starvation, Proc. Natl. Acad. Sci. U. S. A. 106 (2009) 10147–10152.